Application of response surface methodology to optimize the treatment process of high conversion of free fatty acids using (1R)-(-)-camphor-10--sulfonic acid and iron(III) sulphate

Adeeb Hayyan[1,2], Khalid M. Abed[1,3], Mohammed A. Al-Saadi[4], Amal A. M. Elgharbawy[5,6], Yousef Mohammed Alanazi[7], Jehad Saleh[7], Nur Hanie Mohd Latiff[8], Sharifah Shahira Syed Putra[9], Mohd Roslan Mohd Nor[10] and Shareef Fadhil Mahel Alhashemi[11]

[1]*Department of Chemical Engineering, Faculty of Engineering, Universiti Malaya, Kuala Lumpur, Malaysia*
[2]*Sustainable Process Engineering Centre (SPEC), Faculty of Engineering, Universiti Malaya, Kuala Lumpur, Malaysia*
[3]*Department of Chemical Engineering, College of Engineering, University of Baghdad, Baghdad, Iraq*
[4]*National Chair of Materials Science and Metallurgy, University of Nizwa, Nizwa, Oman*
[5]*International Institute for Halal Research and Training (INHART), International Islamic University Malaysia, Kuala Lumpur, Malaysia*
[6]*Bioenvironmental Engineering Research Centre (BERC), Department of Biotechnology Engineering, Faculty of Engineering, International Islamic University Malaysia (IIUM), Kuala Lumpur, Malaysia*
[7]*Department of Chemical Engineering, College of Engineering, King Saud University, Riyadh, Saudi Arabia*
[8]*Global Centre for Environmental Remediation (GCER), College of Engineering, Science, and Environment (CESE), University of Newcastle, Callaghan, Australia*
[9]*Faculty of Industrial Sciences and Technology, Universiti Malaysia Pahang Al-sultan Abdullah, Lebuhraya Tun Abdul Razak, 26300 Gambang, Pahang, Malaysia*
[10]*Halal Research Group, Academy of Islamic Studies, Universiti Malaya, Kuala Lumpur, Malaysia*
[11]*Department of Chemistry, College of Science, Sultan Qaboos University, Muscat, Oman*

Abstract

This study investigates biodiesel production from acidic crude palm oil using one homogeneous catalyst, (1R)-(-)-camphor-10-sulfonic acid (10-CSA), and one heterogeneous catalyst, iron(III) sulphate, focusing on their catalytic activity, recyclability, and process optimisation by using response surface methodology. Optimal conditions were identified by utilising a Box-Behnken factorial design. For 10-CSA, the optimised conditions yielded a free fatty acid (FFA) reduction to 0.43 wt.%, with a catalyst dosage of 1.5 wt.% (investigated range: 1.0-2.0 wt.%), methanol-to-oil molar ratio of 12.67:1 (investigated range: 10 to 14:1), reaction temperature of 59.6 °C (investigated range: 50 to 65 °C), and reaction time of 33.1 min (investigated range: 30 to 40 min). For iron(III) sulphate, the optimised conditions led to FFA reduction to 1.04 wt.%, with a catalyst dosage of 3.14 wt.% (investigated range: 2.5 to 3.5 wt.%), methanol-to-oil molar ratio of 12:1 (investigated range: 10 to 14:1), reaction temperature of 60 °C (investigated range: 55 to 70 °C), and reaction time of 178.6 min (investigated range: 150 to 180 min). Results of the ANOVA analysis confirmed the significance of key factors for both catalysts ($p < 0.05$), with R^2 values of 0.937 for 10-CSA and 0.916 for iron(III) sulphate, indicating strong model fits. The mean relative percent deviation (MRPD) was <5 % for both models, demonstrating high predictive accuracy. The lack of fit was found to be insignificant ($p > 0.05$), confirming the adequacy of the models. Both catalysts achieved high FFA conversions of 95.2 % for 10-CSA and 88.2 % for iron(III) sulphate, which meets the EN 14214 and ASTM D6751 standards. Notably, 10-CSA exhibited superior catalytic activity and recyclability, highlighting its potential for industrial-scale biodiesel production. This study offers practical insights into optimising esterification processes for biodiesel production from acidic crude palm oil.

Keywords: Acidic crude palm oil; biodiesel; esterification; homogeneous acid catalyst; heterogeneous acidic catalyst.

Available on-line at the Journal web address: http://www.ache.org.rs/HI/

ORIGINAL SCIENTIFIC PAPER

UDC: 665.75:622.276.32

Hem. Ind. **00(0)** 000-000 (2025)

Corresponding authors: Adeeb Hayyan, Department of Chemical Engineering, Faculty of Engineering, University Malaya, Kuala Lumpur 50603, Malaysia; E-mail: adeeb.hayyan@yahoo.com
Amal A. M. Elgharbawy, International Institute for Halal Research and Training (INHART), International Islamic University Malaysia, P.O Box 10, 50728 Kuala Lumpur, Malaysia; E-mail: amalgh@iium.edu.my

Paper received: 15 May 2024; Paper accepted: 17 Mach 2025; Paper published: 7 May 2025.
https://doi.org/10.2298/HEMIND240515003H

1. INTRODUCTION

Biodiesel has a superior emission profile compared to diesel, substantially reducing emissions of unburned hydrocarbons, carbon monoxide, sulphates, polycyclic aromatic hydrocarbons, nitrated polycyclic aromatic hydrocarbons, and particulate matter [1-5]. As a result of the limited annual production of crude palm oil and the increasing global market demand, the priority of crude palm oil usage has been given to palm oil refineries for food processing. Acidic crude palm oil (ACPO), produced in palm oil mills, is considered a less favourable variant of crude palm oil due to its association with various operational and processing factors, such as milling inefficiencies, prolonged storage durations, and the effects of climate change [6]. Acidic oil with high free fatty acid (FFA) content has to be submitted to a pretreatment step to remove the FFA before refinery processing or biodiesel production [4,6-11]. Many types of heterogeneous acid catalysts have been used in biodiesel production, such as ferric sulphate and sulphated zirconia [12,13]. In addition, lipases were used as biocatalysts in esterification and transesterification of acidic oils or fats to produce biodiesel [14-16]. However, immobilisation is required to ensure long stability and efficiency of lipases. Homogeneous acid catalysts play a crucial role in biodiesel production, participating in the transesterification process. Thus, these catalysts have been extensively studied due to their effectiveness in facilitating conversion of triglycerides into fatty acid methyl esters. In addition to acidic, alkaline catalysts have also been explored for their potential in biodiesel production [17]. However, different challenges have also been recognised associated with the use of homogeneous catalysts. For instance, the presence of high amounts of FFAs in biodiesel feedstock can lead to issues such as the formation of water and soap, as well as separation problems when using alkaline catalysts, indicating the need for exploration of alternatives to address these limitations [18]. Therefore, research has been directed towards the development and evaluation of novel catalysts for biodiesel production [19]. Recently, ionic liquids and deep eutectic solvents were applied to esterify FFA in acidic oils [20-23]. Among different substances, (1R)-(-)--camphor-10-sulfonic acid (10-CSA) and iron(III) sulphate ($Fe_2(SO_4)_3$) have shown potential to be used in the biodiesel industry due to their catalytic activity and the appearance in solid powder form under normal conditions. 10-CSA has been studied for its catalytic properties in various organic reactions [24] as well as in the synthesis of different materials for potential applications in coatings and composites [25]. Furthermore, the chiral nature of 10-CSA has been explored, highlighting its potential for use in enantioselective processes, which could be beneficial in the production of specific biodiesel compounds [26].

On the other hand, $Fe_2(SO_4)_3$ has been investigated for its role in coagulation processes for the removal of pollutants from water, demonstrating its effectiveness in treating wastewater [27]. Potentials of 10-CSA and $Fe_2(SO_4)_3$ for utilisation in the biodiesel industry are further supported by applications of these compounds in polymerisation processes and their use as calibration standards in spectroscopic techniques [28,29]. These diverse applications demonstrate the multifaceted nature of these compounds and their potential for various processes involved in biodiesel production. Thus, catalytic properties, environmental interactions, and diverse applications in organic synthesis and industrial processes make 10-CSA and $Fe_2(SO_4)_3$ attractive for further investigations.

Hence, this study aims to optimise and compare the catalytic activity of a homogeneous acid catalyst (10-CSA) and a heterogeneous acidic catalyst ($Fe_2(SO_4)_3$) for esterification of ACPO and biodiesel production using a Box-Behnken factorial design. The aim was to perform a novel comparative analysis to provide insights into the performance of these catalysts under similar reaction conditions. The design explores the effects of catalyst dosage, methanol-to-oil molar ratio, reaction temperature, and reaction time on biodiesel outcomes. By optimising these factors, the study seeks to develop efficient biodiesel production methods that meet the EN 14214 and ASTM D6751 standards, addressing challenges posed by ACPO and guiding industrial-scale biodiesel production from lower-quality feedstock. This study's findings are intended to primarily aid the transportation sector by providing a renewable alternative to conventional diesel fuel, particularly for vehicle fuel, marine transport, as well as agricultural and construction equipment.

2. MATERIALS AND METHODS

2. 1. Chemicals and materials

Acidic crude palm oil (ACPO) was obtained from a local palm oil mill in Selangor Darul Ehsan, Malaysia. Laboratory-grade methanol 99.8 % was purchased from Merck (Malaysia). Iron(III) sulphate ($Fe_2(SO_4)_3$) (reagent grade 97 %) was

purchased from R&M Chemicals (Malaysia). (1R)-(-)-camphor-10-sulfonic acid (10-CSA) (ACS grade 99 %) was purchased from Merck (Malaysia).

2. 2. Esterification (production of biodiesel from acidic crude palm oil)

The arbitrary amount of ACPO was first heated in an oven at 70 °C. The reactor system was maintained at the desired temperature by adjusting the temperature of the circulating water bath. Next, 30 g of ACPO was measured and poured into a multi-unit batch reactor, with each unit having a 1 dm^3 volume. Mechanical stirring was used to ensure homogeneity, while atmospheric pressure was maintained by an automated control system. In specific, all experiments were carried out in a laboratory scale batch multi-unit reactor system with methanol reflux, with a jacketed vessel connected to a circulating bath. The reaction temperature and stirring speed were monitored by uniquely designed feedback controllers. The catalyst was mixed with methanol before being added to the reactor. When using 10-CSA as the catalyst, the catalyst dosage ranged from 0.25 to 2.25 wt.%, while the methanol-to-oil molar ratio varied from 2 to 14, requiring 2.17 to 15.18 g of methanol. When using iron(III) sulphate, the catalyst dosage ranged from 2 to 6 wt.%, while the methanol-to-oil molar ratio ranged from 8 to 12, requiring 8.68 to 13.02 g of methanol. The reactor was then connected to a reflux condenser and magnetic stirring was adjusted to 450 rpm. At the same time, the reaction time was recorded using a stopwatch. After each experimental run (Supplementary material, Tables S1 and S2), the product was left to settle by gravity and the excess methanol was evaporated in the oven. The FFA content of the treated ACPO was determined and reported for each experiment. The optimal conditions for ACPO esterification were verified by repeating three validation experiments. The last section of this study was characterisation of the produced biodiesel. The biodiesel quality was checked for its compliance with specifications in the EN 14214 and ASTM D6751 standards for biodiesel. The FFA content of ACPO was determined based on the American Oil Chemist's Society (AOCS) official method Ca 5a-40 commercial fats and oils [19,30]. The ester content, mono, di and triacylglycerols, and free and total glycerol contents were determined using a gas chromatography flame ionisation detector (GC/FID) (Perkin Elmer Clarus 500, Netherlands).To measure the methyl ester (biodiesel) content in the sample, different concentrations of the diluted standard (FAME C14-C18) mixed with *n*-hexane were injected into the GC column respectively using splitless mode injector with a capillary column (SP 2330 polar column ID: 0.32mm). Helium was used as a carrier gas at a flow rate of 1 cm^3 min^{-1}, and each sample run time was approximately 40 min, starting at 50 °C for about 1 min and subsequently increased to 220 °C at 2 °C min^{-1} and held at this temperature for 10 min. Approximately 1 µL of the sample was diluted with *n*-hexane before being injected into the GC. The weights of biodiesel produced were determined by comparing them to the sample of pure standards [31]. The yield, % of biodiesel was calculated by following Equation (1):

$$\text{Yield} = (\text{Total weight of biodiesel}/\text{Total weight of oil in the sample}) \times 100 \quad (1)$$

2. 3. Optimisation method

Response surface methodology (RSM) was employed to determine optimal operating conditions for ACPO esterification performed with the use of the investigated homogeneous and heterogeneous catalysts. A Box-Behnken factorial design with four factors and three levels was selected for this study, comprising 29 factorial points and five centre points to enhance robustness. The four factors were catalyst dosage, methanol-to-oil molar ratio, reaction temperature, and reaction time. Table 1 presents the specific values for these factors when 10-CSA was used as the homogeneous catalyst, while Table 2 provides the same information for the heterogeneous catalyst ($Fe_2(SO_4)_3$).

Table 1. *Experimental range and levels of the factors for (1R)-(-)-camphor-10-sulfonic acid*

Factor	Symbols	Range and levels		
		-1	0	1
Catalyst dosage, wt.%	*A*	0.25	1.25	2.25
Methanol-to-oil molar ratio	*B*	2	8	14
Reaction temperature, °C	*C*	40	60	80
Reaction time, min	*D*	10	30	50

Table 2. *Experimental range and levels of the factors for iron (III) sulphate*

Factor	Symbols	Range and levels		
		-1	0	1
Catalyst dosage, wt.%	*A*	2	4	6
Methanol-to-oil molar ratio	*B*	8	10	12
Reaction temperature, °C	*C*	60	70	80
Reaction time, min	*D*	100	150	200

A second-order response surface was derived to describe the esterification process with general Equation (2):

$$F = \alpha_0 + \alpha_1 A + \alpha_2 B + \alpha_3 C + \alpha_4 D + \alpha_{12} AB + \alpha_{13} AC + \alpha_{14} AD + \alpha_{23} BC + \alpha_{24} BD + \alpha_{34} CD + \alpha_{11} A^2 + \alpha_{22} B^2 + \alpha_{33} C^2 + \alpha_{44} D^2 \quad (2)$$

where, *F* / wt.% represents the FFA content of the treated ACPO, whereas, for $Fe_2(SO_4)_3$, the objective function was transformed to represent ln the FFA content (ln *F*).

The transformation was used to achieve a more significant model fit. In this model, α_0 is the intercept term, α_1, α_2, α_3, and α_4 are linear coefficients, α_{12}, α_{13}, α_{14}, α_{23}, α_{24}, and α_{34} are interactive coefficients, α_{11}, α_{22}, α_{33}, and α_{44} are quadratic coefficients, and *A, B, C,* and *D* represent the actual factors, which are catalyst dosage, methanol-to-oil molar ratio, reaction temperature, and reaction time, respectively. Experimental data analysis and response surface plotting were conducted using Design-Expert software (version 12.0.3.3, Stat-Ease Inc., MN) [31,32]. Table S1 (Supplementary material) provides the Box-Behnken design used for optimising 10-CSA-catalyzed esterification, while Table S2 (Supplementary material) presents the design for optimising ($Fe_2(SO_4)_3$)-catalysed esterification.

3. RESULTS AND DISCUSSION

3. 1. Optimization of the process using (1R)-(-)-camphor-10-sulfonic acid

Optimisation of biodiesel production using (1R)-(-)-camphor-10-sulfonic acid was performed by investigating the effects of catalyst dosage, methanol-to-oil molar ratio, reaction temperature, and reaction time on FFA reduction and conversion efficiency. Furthermore, the first step in analysing the results involved creating a predictive model using response surface methdology (RSM) with the Box-Behnken factorial design. This design allows for the systematic evaluation of the key factors affecting esterification, stated above. A quadratic regression model for 10-CSA was derived from the experimental data, and the following equation was obtained (Equation 3):

$$\ln F = 0.3364 - 0.6454A - 0.5751B - 0.1076C - 0.3463D - 0.5016AB + 0.0275AC - 0.2036AD - 0.0410BC - 0.1488BD - 0.0154CD + 0.2870A^2 + 0.2208B^2 + 0.2843C^2 + 0.1707D^2 \quad (3)$$

Results of the ANOVA analysis for the response surface quadratic model for 10-CSA is presented in Table 3. The RSM application yielded a statistically significant quadratic model for optimising FFA conversion (*F*-value = 46.67, p <0.0001), with only a 0.01 % probability that the observed variance could arise from noise. The model's high adjusted R^2 (0.918) and predicted R^2 (0.877) values demonstrated excellent agreement, confirming its strength in predicting FFA conversion within the experimental design space. Moreover, the model's strong signal-to-noise ratio (adequate precision = 25.442) validated its utility for process optimisation.

Catalyst dosage (*A*) and methanol-to-oil molar ratio (*B*) emerged as the most influential factors, with exceptionally high *F*-values of 254.15 and 201.79, respectively (p <0.0001). Reaction time (*D*) also exhibited a significant impact (*F* = 73.14, p <0.0001), while reaction temperature (*C*) showed moderate significance (*F*-value = 7.06, p = 0.0110). Quadratic terms for all factors (A^2, B^2, C^2, D^2; p <0.01) further highlighted nonlinear relationships between the variables and FFA conversion, suggesting the presence of optimal operating conditions beyond which the response plateaus or declines.

Significant interactions were observed between the catalyst dosage and methanol-to-oil ratio (*AB*; *F*-value = 51.17, p <0.0001), catalyst dosage and reaction time (*AD*; *F*-value = 8.43, p = 0.0058), and methanol-to-oil ratio and reaction time (*BD*; *F*-value = 4.50, p = 0.0397). The strong *AB* interaction implies synergistic effects, where increasing both catalyst dosage and methanol-to-oil ratio enhances FFA conversion more than their individual contributions. Conversely, interactions involving temperature (*AC*, *BC*, *CD*) were statistically insignificant (p >0.05), indicating negligible combined effects with other variables.

While higher catalyst dosages initially improve conversion rates, diminishing returns may occur at elevated levels due to potential saturation effects. Similarly, excessive methanol-to-oil ratios could dilute reactant concentrations or increase operational costs without proportional gains in FFA reduction.

While the methanol-to-oil ratio (*B*) is generally significant, the quadratic term for temperature (C^2, +0.2843) indicates that its effect becomes more pronounced near the reference point. This nonlinearity suggests that the temperature influence intensifies within specific operational ranges, potentially overshadowing the methanol-to-oil ratio (*B*) in localised regions of the design space. Thus, around the reference conditions, catalyst dosage (*A*) and temperature (*C*) may dominate due to curvature effects, even though the methanol-to-oil ratio (*B*) remains critical overall.

Table 3. *ANOVA analysis for the response surface quadratic significant model for (1R)-(-)-camphor-10-sulfonic acid*

Source	Sum of squares	Degree of freedom	Mean square	*F*-value	*p*-value
Model	25.70	14	1.840	46.670	< 0.0001
A	10.00	1	10.00	254.150	< 0.0001
B	7.940	1	7.940	201.790	< 0.0001
C	0.278	1	0.277	7.060	0.0110
D	2.880	1	2.880	73.140	< 0.0001
AB	2.010	1	2.010	51.170	< 0.0001
AC	0.006	1	0.006	0.153	0.6972
AD	0.332	1	0.332	8.430	0.0058
BC	0.013	1	0.013	0.342	0.5618
BD	0.177	1	0.177	4.500	0.0397
CD	0.002	1	0.002	0.048	0.827
A^2	1.070	1	1.070	27.170	< 0.0001
B^2	0.633	1	0.633	16.080	0.0002
C^2	1.050	1	1.050	26.650	< 0.0001
D^2	0.378	1	0.378	9.610	0.003
Residual	1.690	43	0.039		
Pure error	0.016	33	0.001		

The perturbation plot (Figure S1) shows that the catalyst dosage (*A*) and methanol-to-oil molar ratio (*B*) have the strongest influence on FFA conversion during 10-CSA-catalysed esterification, as indicated by their steeper curves. Reaction temperature (*C*) and reaction time (*D*) have less impact, with flatter curves, highlighting the critical role of catalyst dosage and methanol-to-oil ratio in optimising FFA conversion.

From Figure S2, the diagnostic plots confirm the robustness of the quadratic model. The normal plot of residuals demonstrates that residuals align closely with a straight line, indicating adherence to a normal distribution. The residual *vs*. predicted plot exhibits a random scatter of points, suggesting homoscedasticity (constant variance) across the range of predicted values. The Box-Cox plot reveals that the current transformation parameter in the Box-Cox transformation, used to identify the most appropriate transformation of the response variable to stabilize variance and improve normality (λ) of 1 lies within the confidence interval for the optimal λ (0.57), implying that transformation of the response variable is not necessary [33]. Furthermore, the Cook's distance plot indicates that there are not influential outliers that significantly distort the model, as most data points exhibit low Cook's distances. Collectively, these diagnostics validate the model's assumptions of normality, constant variance, and absence of influential outliers, confirming its reliability for predicting FFA conversion [34].

The response surface plots (Fig. 1) elucidate the effects of key factors and their interactions on FFA reduction. At a constant reaction temperature of 60 °C and reaction time of 30 min, increasing both catalyst dosage and methanol-to-oil molar ratio significantly reduced the FFA content. This synergistic effect underscores the critical role of these factors in driving the esterification reaction. Higher methanol-to-oil ratios likely shift the reaction equilibrium toward ester formation, while increased catalyst dosages enhance reaction kinetics. Meanwhile**,** at a fixed methanol-to-oil molar ratio of 8:1 and reaction time of 30 min, the effect of reaction temperature was significant but less pronounced compared to the catalyst dosage. The lack of a significant interaction between the catalyst dosage and temperature suggests that temperature variations have a limited impact on FFA reduction within the studied range. Additionally**,** a constant methanol-to-oil molar ratio of 8:1 and reaction temperature of 60 °C, longer reaction times and higher catalyst

dosages synergistically improved FFA reduction. This highlights the importance of optimising both parameters to maximise the conversion efficiency.

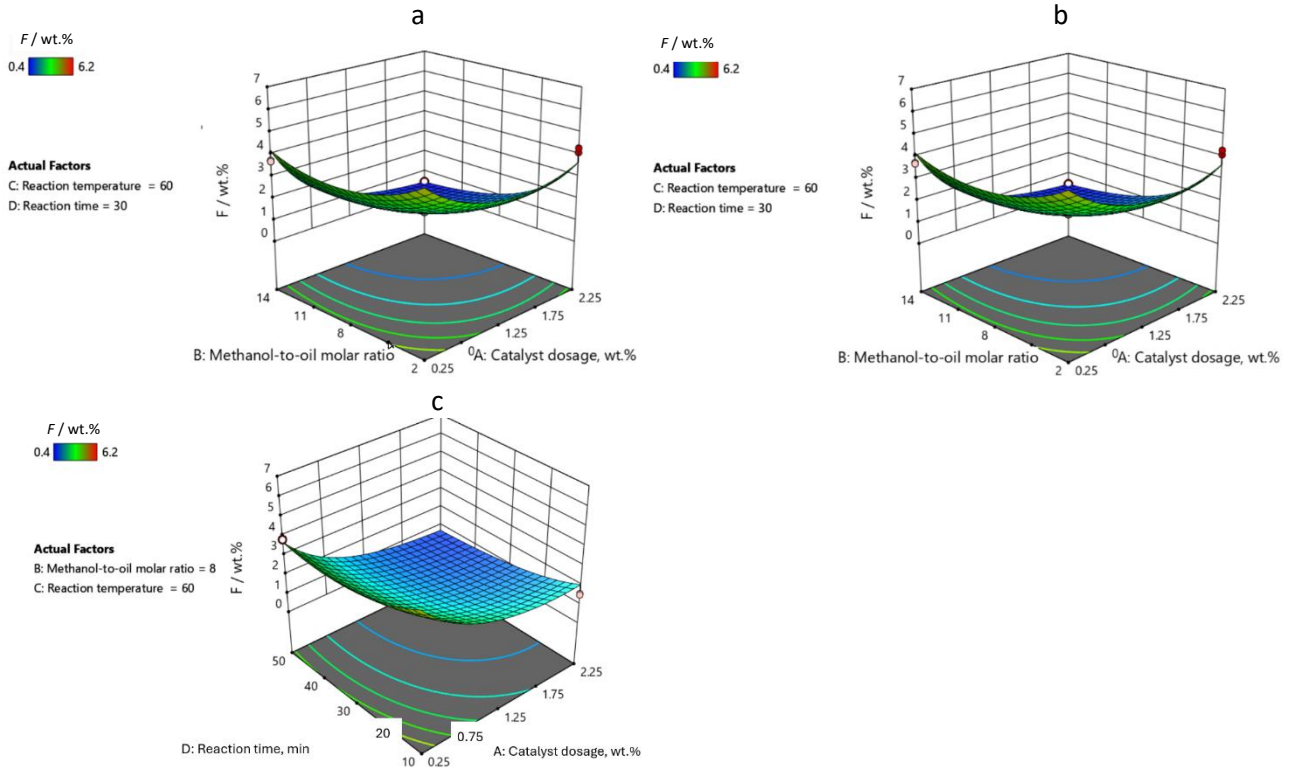

Figure 1. *3D response surface plots of the effect of 10-CSA on the FFA reduction as a function of: (a) catalyst dosage and methanol-to-oil molar ratio, (b) catalyst dosage and reaction temperature, (c) catalyst dosage and reaction time. The other factors were held at zero level.*

The contour plots (Fig. S3, Supplementary material) provide a clear visualisation of the response surface, enabling the identification of optimal operating conditions. For instance, the steep gradients in the contour lines confirm the strong influence of these factors on FFA reduction. Moreover, the relatively flat contour lines suggest that these factors have a more moderate impact, consistent with their lower F-values in the ANOVA analysis.

A set of constraints was applied to determine the optimal conditions for 10-CSA -catalysed esterification. Table S3 (Supplementary material) outlines the optimisation constraints, and Table S4 (Supplementary material) shows the resulting optimised solution. The optimal conditions for this process were a catalyst dosage of 1.5 wt.%, a methanol-to-oil molar ratio of 12.67:1, a reaction temperature of ~60 °C, and a reaction time of 33.11 min, resulting in an FFA content of 0.43 wt.% . These optimal conditions align with previous studies that emphasise the importance of catalyst dosage and methanol-to-oil molar ratio in driving esterification.

Several studies have investigated the impact of these parameters on FFA production and have identified optimal conditions. The significance of catalyst dosage and solvent effect in achieving high conversion and selectivity to FFA has been demonstrated by Jia *et al.* [35] realising 100 % conversion and 96.5 % selectivity to FFA at the optimal catalyst content and in methanol as a solvent. Furthermore, Xie *et al.* [36] highlighted the impact of catalyst dosage, methanol-to-oil molar ratio, and reaction temperature on FFA conversion to biodiesel. The study demonstrated that under specific operational conditions, including a methanol/oil molar ratio of 30:1, a catalyst dosage of 5 wt.%, a reaction temperature of 140 °C, and a reaction duration of 8 h, a high oil conversion of 92.2 % was achieved with total FFA transformation to biodiesel. The current study demonstrated good results at a lower conversion temperature, which is more suitable for industry.

Production of biodiesel from feedstock with high FFA contents often requires the use of solid catalysts to reduce FFA levels and ensure high biodiesel yields. Faruque *et al.* [37] utilised sulphated zirconia as a solid acid heterogeneous catalyst for biodiesel production from Neem oil, achieving a 95 % biodiesel yield while maintaining a 9:1 methanol-to-oil ratio. Solid acid catalysts have been preferred for high FFA esterification due to their insensitivity to the FFA content,

elimination of the need for a biodiesel washing step, ease of catalyst separation, and lower product contamination levels. Additionally, solid acid catalysts are less corrosive, produce less waste, and are easier to separate from reactants and products, making them preferable over hazardous mineral acids for high FFA esterification [38]. Furthermore, the economic benefit of using solid catalysts in biodiesel production lies in their reusable nature for low-quality feedstock, leading to cheaper production costs [39]. The use of solid catalysts for biodiesel production has also been explored in the context of specific feedstock. For instance, efficient conversion of low-grade, nonedible oil feedstock into biodiesel was demonstrated using pumice as a bifunctional solid catalyst, which can catalyse the esterification of FFA and transesterification of fatty acid glycerides simultaneously [40]. This highlights the versatility of solid catalysts in enabling the conversion of diverse feedstocks into biodiesel.

3. 2. Optimisation of the process using iron(III) sulphate

Optimisation of biodiesel production using iron (III) sulphate was performed by evaluating the effects of (a) catalyst dosage, (b) methanol-to-oil molar ratio, (c) reaction temperature, and (d) reaction time on FFA reduction and conversion efficiency. A quadratic regression model for this process was derived in a similar manner as for that catalysed by 10-CSA, focusing on the key factors impacting esterification (Eq. 4):

$$\begin{aligned}\ln F = {} & -0.332888 + -0.645336A + -0.563832B + -0.110702C + -0.347448D + -0.485991AB + \\ & + 0.0219763AC + -0.209352AD + -0.0303575BC + -0.159192BD + -0.0119114CD + \\ & + 0.289957A^2 + 0.224655B^2 + 0.288779C^2 + 0.172073D^2\end{aligned} \quad (4)$$

The quadratic model (Table 4) developed for the second catalyst exhibited statistical significance (F-value = 45.71, p <0.0001), with the catalyst dosage (F-value = 251.85, p <0.0001) and methanol-to-oil molar ratio (F-value = 192.25, p<0.0001) emerging as the dominant factors influencing FFA reduction.

Table 4. *ANOVA analysis for the response surface quadratic significant model for iron(III) sulphate*

Source	Sum of squares	Degree of freedom	Mean square	*F*-value	*p*-value
Model	25.390	14	1.810	45.71	< 0.0001
A	10.00	1	10.00	251.85	< 0.0001
B	7.630	1	7.630	192.25	< 0.0001
C	0.294	1	0.294	7.41	0.0093
D	2.900	1	2.900	73.00	< 0.0001
AB	1.890	1	1.890	47.61	< 0.0001
AC	0.004	1	0.004	0.097	0.7565
AD	0.351	1	0.351	8.83	0.0048
BC	0.007	1	0.007	0.186	0.6686
BD	0.203	1	0.203	5.11	0.0289
CD	0.001	1	0.001	0.029	0.8665
A^2	1.090	1	1.090	27.48	< 0.0001
B^2	0.655	1	0.655	16.50	0.0002
C^2	1.080	1	1.080	27.26	< 0.0001
D^2	0.384	1	0.384	9.68	0.0033
Residual	1.710	43	0.039		
Pure Error	0.007	33	0.0002		

Reaction time (F-value =73.00, p <0.0001) and temperature (F-value = 7.41, p = 0.0093) also contributed significantly, albeit to a lesser extent. Synergistic interactions were observed between the catalyst dosage and methanol ratio (*AB*, p <0.0001), catalyst dosage and reaction time (*AD*, p=0.0048), and methanol-to-oil molar ratio and reaction time (*BD*, p = 0.0289), highlighting the interconnected roles of these parameters in driving esterification efficiency. The significant quadratic terms (A^2, B^2, C^2, D^2; p <0.01) confirmed nonlinear relationships, suggesting the existence of optimal operating conditions beyond which FFA reduction plateaus. Despite a significant lack of fit (p <0.0001), the model demonstrated strong predictive capability, as evidenced by the high adjusted, R^2 = 0.916, and predicted, R^2 = 0.874, along with an exceptional signal-to-noise ratio (adequate precision is 25.045). The natural log transformation of the response variable (λ = 1) aligned with the Box-Cox recommendation λ = 0.57), validating the model's stability. These results underscore

the catalyst's sensitivity to dosage and methanol-to-oil molar ratio, with temperature and time acting as secondary levers, and provide a reliable framework for optimising FFA conversion in industrial applications.

While temperature-related factors are generally significant, their local influence near the reference point is reduced due to the nonlinear response surface behaviour, where the effect plateaus, and the process becomes less sensitive to temperature variations within that narrow range.

The perturbation plot (Fig, S4, Supplementary material) for the $Fe_2(SO_4)_3$-catalysed esterification process illustrates the sensitivity of FFA content to changes in process factors at the reference point: catalyst dosage of 1.25 wt.%, methanol-to-oil molar ratio of 8:1, reaction temperature of 60 °C, and reaction time of 30 min. Increasing the catalyst dosage from the reference point significantly reduces the FFA percentage, highlighting its critical role in esterification efficiency. The methanol-to-oil molar ratio also influences FFA reduction but to a slightly lesser extent. Reaction temperature and reaction time exhibit flatter slopes, indicating minimal effects on FFA content within the studied range. Overall, for the $Fe_2(SO_4)_3$ catalyst, the catalyst dosage stands out as the most significant factor affecting esterification, followed by the methanol-to-oil molar ratio, as confirmed by their high F-values. While the perturbation plot shows minimal temperature influence near the reference point, Equation (4) and the ANOVA results (*F-value* = 7.41, $p = 0.0093$) indicate that temperature-related factors significantly affect FFA content across the broader experimental range. This suggests that the effect of temperature becomes more pronounced at conditions further from the reference point, likely due to nonlinear interactions captured by the quadratic term (C^2).

A normal plot of residuals was utilised to confirm the distribution of residuals associated with the esterification process facilitated by $Fe_2(SO_4)_3$ (Fig. S5, Supplementary material). This analytical step is crucial for affirming that the residuals follow a normal distribution, a key assumption for the validity of subsequent statistical analysis [41]. The graph demonstrated that the data points, signifying the externally studentised residuals, were in close proximity to the theoretical line that represents a normal distribution. Such proximity lends support to the normality premise for the statistical evaluations applied in our model. Notably, while a minor number of data points stray from this theoretical line, the magnitude of their divergence falls within permissible ranges and does not suggest any underlying issues with the model, like heteroscedasticity or nonlinear dynamics. These residuals are differentiated by FFA values, indicating the non-existence of a discernible connection between the magnitude of residuals and FFA concentrations. The absence of a discernible pattern reinforces the integrity of our statistical model, indicating that the projections made from the $Fe_2(SO_4)_3$-catalyzed esterification process stand on a firm statistical foundation suitable for drawing inferences. The 3D surface plots (Fig. 2) and contour plots (Fig. S6, Supplementary material) reveal significant interactions between key process variables affecting FFA reduction during the esterification process.

The catalyst dosage and methanol-to-oil molar ratio exhibit the most pronounced effects, with optimal FFA reduction achieved at higher catalyst dosages (1.5 to 2.25 wt.%) and methanol-to-oil molar ratios (10-14). Similarly, increasing both catalyst dosage and reaction time (40 to 50 min) leads to greater FFA reduction, while the reaction temperature (60 to 80 °C) has a moderate influence.

Based on these findings, the optimal conditions for maximising FFA reduction are identified as a catalyst dosage of 1.5 to 2.25 wt.%, methanol-to-oil molar ratio of 10-14, reaction temperature of 60 to 80 °C, and reaction time of 40 to 50 min. Operating within these ranges ensures efficient FFA conversion while minimising resource consumption.

Table S5 (Supplementary material) outlines the optimisation constraints and Table S6 (Supplementary material) shows the optimised solutions for $Fe_2(SO_4)_3$-based esterification, with a focus on the catalyst dosage, methanol-to-oil molar ratio, reaction temperature, reaction time, and the corresponding FFA content.

The best solution uses a catalyst dosage of 3.14 wt.%, a 12:1 methanol-to-oil molar ratio, a temperature of 60 °C, and a reaction time of 178.59 min. This setup results in an FFA content of 1.04 % with FFA conversion of 88.2 % with a desirability score of 0.77, indicating how well the solution aligns with the desired outcomes. The similar desirability scores across other solutions suggest that small changes in the catalyst dosage and reaction time can impact the final FFA content, with this particular combination showing a high level of optimisation. The data suggest that the catalyst dosage is a key factor in achieving effective esterification. Variations in this parameter can influence the balance between efficient FFA reduction and the risk of overusing the catalyst, which can increase costs or impact sustainability. The consistent desirability scores across multiple solutions point to the robustness of the optimisation process.

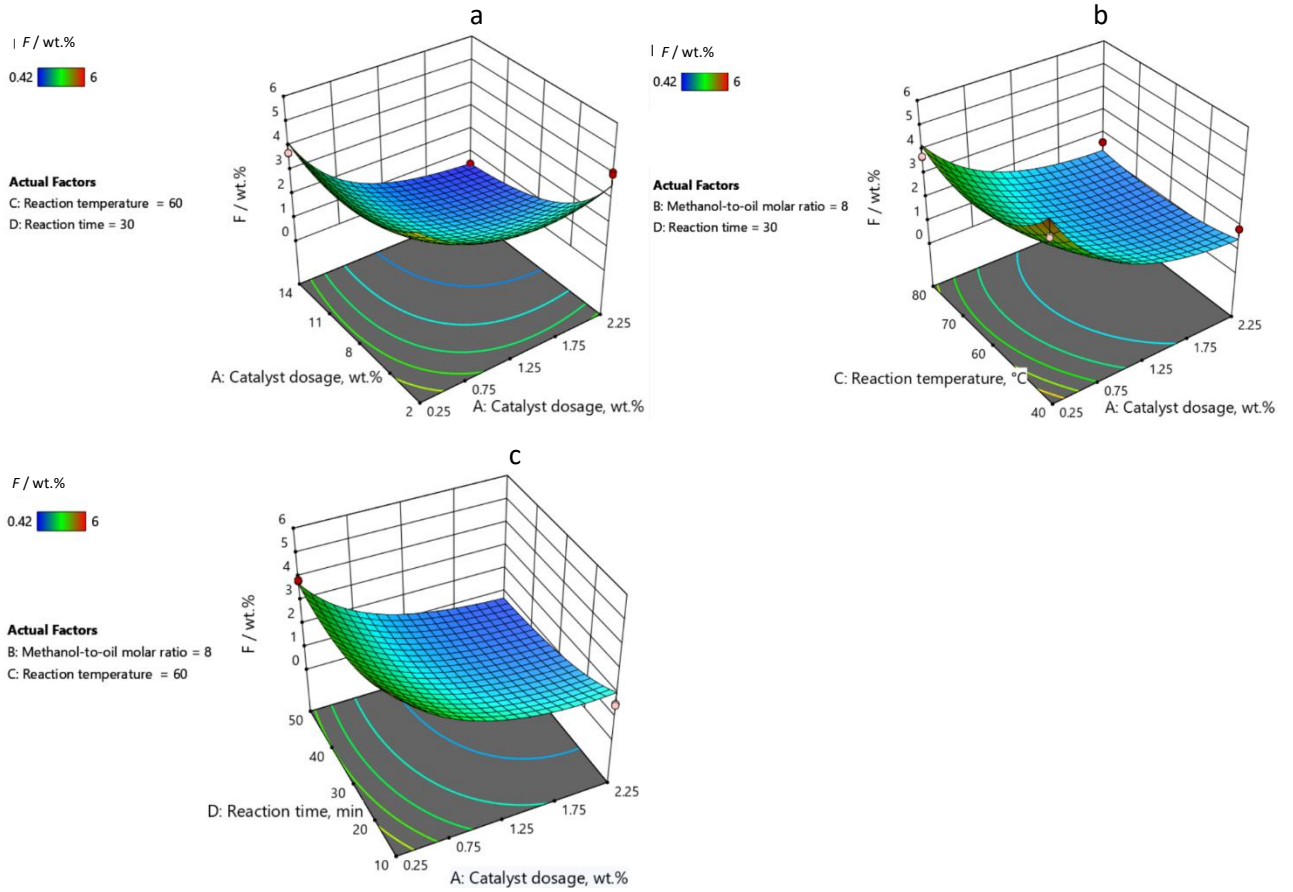

Figure 2. *3D response surface plots of the effect of $Fe_2(SO_4)_3$ on the FFA reduction as a function of: (a) catalyst dosage and methanol-to-oil molar ratio, (b) catalyst dosage and reaction temperature, (c) catalyst dosage and reaction time. The other factors were held at zero level*

3.3. Physicochemical properties of biodiesel produced from acidic crude palm oil

Table S7 (Supplementary material) outlines the specifications for biodiesel derived from ACPO with the use of $Fe_2(SO_4)_3$ as a catalyst, comparing the results with standards like EN 14214 and ASTM D6751. The biodiesel meets or exceeds the key industry requirements, including the ester content, monoacylglycerol content, diacylglycerol content, and total glycerol content under a catalyst dosage of 1.5 wt.%, a methanol-to-oil molar ratio of 12.67:1, a reaction temperature of 59.6 °C, and a reaction time of 33.1 min.

The biodiesel exhibited a molar ester percentage of 96.3 %, slightly below the EN 14214 minimum requirement of 96.5 %, but still indicative of high conversion efficiency. The contents of monoacylglycerols (0.05 wt.%), diacylglycerols (0.025 wt.%), and triacylglycerols (<0.01 wt.%) were significantly lower than the maximum limits set by EN 14214, indicating efficient transesterification. Both free glycerol (<0.01 wt.%) and total glycerol (0.050 wt.%) contents met the stringent limits of EN 14214 and ASTM D6751, reflecting high product purity. The water content (473 mg kg^{-1}) complied with both standards, ensuring good fuel stability. Metal contaminants, including potassium (1 mg kg^{-1}) and phosphorus (7.10 mg kg^{-1}), were well within permissible limits, minimising risks of engine deposits. The biodiesel density (86 kg m^{-3}), flash point (182 °C), and sulphated ash (<0.005 %) satisfied the respective EN and ASTM requirements, ensuring safe storage and combustion characteristics. Additionally, it exhibited a low total contamination (0.008 mg kg^{-1}) and achieved a Class 1 rating in the copper strip corrosion test, confirming excellent oxidative stability and corrosion resistance. Low levels of free glycerol and sulphated ash indicate a high level of purity in the final product. The water content, although close to the maximum limit, remains within acceptable boundaries, suggesting effective control of moisture during production.

The flashpoint, a critical safety measure, significantly exceeds the minimum requirements, indicating safe handling and storage. However, the cloud point of 16 °C could be a concern in colder climates, where biodiesel may solidify more

readily than the conventional diesel. This could require additional measures or additives to ensure performance in diverse conditions. These findings suggest that the optimised conditions for $Fe_2(SO_4)_3$-based esterification yield a product that aligns with industry standards, indicating its potential for large-scale biodiesel production. However, further work may be needed to address the cloud point and other cold-weather properties for broader applicability.

Heterogeneous catalysis in biodiesel production was investigated in other studies reported in the literature. For example, Loryuenyong *et al.* [42] optimised the production of a heterogeneous $Fe_2(SO_4)_3$-calcium oxide/activated charcoal catalyst for biodiesel synthesis. Furthermore, the use of iron-based catalysts has been explored in the production of biodiesel from various feedstocks, such as waste cooking oils [43].

Several studies have investigated the optimal conditions for FFA reduction, providing valuable insights into the influence of catalyst dosage and reaction time on the esterification process. Betiku *et al.* [44] demonstrated the reduction of FFA content from ~28.8 to ~0.4 wt.% using a methanol/FFA molar ratio of 46:1, ferric sulphate dosage of 12 wt.%, and a reaction time of 75 min. Similarly, another study [45] has found that a 19.8:1 methanol-to-FFA molar ratio was effective only within an FFA range of 15 to 25 wt.%, whereas 5 wt.% sulphuric acid showed better performance, working effectively within the FFA range of 15 to 35 wt.%. Furthermore, an artificial neural network-genetic algorithm (ANN-GA) and RSM was utilised to establish the optimum reduction of FFA to 0.58 wt.% with a methanol/NSO molar ratio of 18.51, ferric sulphate dosage of 6 wt.%, and a reaction time of 62.8 min [46]. This emphasises the significance of considering both catalyst dosage and reaction time in tandem to achieve the desired FFA content.

These studies collectively emphasise the critical role of catalyst dosage and reaction time in FFA reduction during biodiesel production. By carefully optimising these parameters, it is possible to achieve significant reductions in the FFA content, ultimately contributing to the production of high-quality biodiesel.

3. 4. Recyclability of the catalysts

Table S8 (Supplementary material) illustrates recyclability of the catalysts used in the present study. The results suggest that homogeneous catalysts, such as 10-CSA, demonstrated higher catalytic activity during recycling runs compared to $Fe_2(SO_4)_3$. This observation suggests that homogeneous acids may be more suitable for industrial-scale biodiesel production due to their consistent catalytic activity and potential for reuse in multiple reaction cycles [47]. The difference in catalytic effectiveness between 10-CSA and $Fe_2(SO_4)_3$ can be attributed to the fundamental characteristics distinguishing homogeneous and heterogeneous catalysts. Homogeneous acid-based catalysts tend to distribute evenly throughout the reaction mixture, resulting in a broader reactive site. This trait likely accounts for their higher initial catalytic efficiency and better recyclability [48]. Conversely, heterogeneous acids may exhibit declining catalytic performance over time due to fouling, leaching, or structural changes [49]. Moreover, separating and purifying the biodiesel was challenging due to the presence of residual catalysts, unreacted methanol, and by-products, which made achieving high purity and process efficiency difficult, especially during recyclability studies.

Data from Table S8 (Supplementary material) indicate that the reduction in FFA content and conversion to FFA with 10-CSA is more consistent over multiple recycling runs compared to those achieved with $Fe_2(SO_4)_3$. FFA reduction with 10-CSA improves with each run, but the rate of FFA conversion from an initial high value tends to decrease over the recycling runs, possibly indicating a decrease in catalytic effectiveness. $Fe_2(SO_4)_3$ shows a more significant decline, suggesting its limitations in maintaining catalytic activity over repeated use [50]. These findings imply that homogeneous catalysts, like 10-CSA, could be better suited for large-scale biodiesel production due to their ability to retain catalytic activity over multiple uses, reducing the need for frequent catalyst replacement, thereby lowering production costs [51].

On the other hand, $Fe_2(SO_4)_3$ performance declines as the number of recycling runs increases, suggesting that it may not be ideal for industrial-scale production. This decrease could lead to increased expenses due to more frequent catalyst replacements or additional measures to rejuvenate the catalyst activity [52]. Given the obtained results, future research could focus on enhancing the recyclability of homogeneous catalysts to maintain high catalytic activity and stable FAME conversion rates over time. This might involve modifying the catalyst chemical structure to reduce degradation or developing methods to restore the catalyst effectiveness after repeated use. Studies might also examine the potential benefits of combining homogeneous and heterogeneous catalysts to capitalise on the strengths of each

type, which could lead to a more efficient and sustainable biodiesel production process [43]. In summary, the obtained results suggest that homogeneous catalysts, particularly10-CSA, could be beneficial for improving the sustainability and efficiency of biodiesel production. Further research into catalyst optimisation and design could bolster robustness and scalability in this industry.

4. CONCLUSION

The ACPO esterification process using 10-CSA and $Fe_2(SO_4)_3$ as a homogenous and heterogeneous catalyst, respectively, was optimised by using RSM. The optimal conditions for 10-CSA were a catalyst dosage of 1.5 wt.%, a methanol-to-oil molar ratio of 12.67:1, a reaction temperature of 59.6 °C, and a reaction time of 33.1 min. These conditions reduced the FFA content to 0.41 wt.% and achieved a FFA conversion rate of 95.14 %. For $Fe_2(SO_4)_3$, the best conditions were a catalyst dosage of 3.14 wt.%, a methanol-to-oil molar ratio of 12:1, a reaction temperature of 60 °C, and a reaction time of 178.6 min, resulting in an FFA reduction to 0.99 wt.% and a FFA conversion of 95.2 % for 10-CSA and 88.2 % for iron(III) sulphate. These findings suggest that 10-CSA is the preferred homogeneous catalyst for large-scale biodiesel production due to several key benefits: its stable solid form, faster reaction times compared to $Fe_2(SO_4)_3$, and greater catalytic activity. Its ability to maintain performance over multiple use points to its cost-effectiveness and sustainability for industrial-scale operations. However, potential challenges encountered during the study include the difficulties in separating and purifying the final biodiesel product to ensure high purity and process efficiency. Therefore, future research should focus on improving separation and purification techniques in homogenous catalysis for biodiesel production. The present study primarily focused on optimising the biodiesel production process rather than catalyst separation. The findings highlight the key process parameters that enhance efficiency and yield, providing valuable insights for improving large-scale biodiesel production.

SUPPLEMENTARY MATERIAL

Additional data are available electronically at https://www.ache-pub.org.rs/index.php/HemInd/article/view/1343, or from the corresponding author on request.

Author contributions: *Adeeb Hayyan: Conceptualization, Supervision, Writing - original draft; Khalid M Abed: Writing - review & editing; Mohammed A. Al-Saadi: Investigation, Writing - original draft; Amal A. M. Elgharbawy: Data curation, Writing - review & editing; Yousef M. Alanazi: Funding acquisition; Jehad Saleh: Funding acquisition; Nur Hanie MohdLatiff: Writing - review & editing; Sharifah Shahira Syed Putra: Writing - review & editing; Mohd RoslanMohd Nor: Resources; Shareef Fadhil MahelAlhashemi: Funding acquisition, Resources.*

Acknowledgement: *This study was supported by the Project Number (RSP2025R511), King Saud University, Riyadh, Saudi Arabia.*

REFERENCES

[1] Sani YM, Daud WMAW, Abdul Aziz AR. Solid acid-catalyzed biodiesel production from microalgal oil - The dual advantage. *J Environ Chem Eng*. 2013; 1(3): 113-121. https://doi.org/10.1016/j.jece.2013.04.006

[2] Akpan IO, Edeh I, Uyigue L. A Review on Biodiesel Production. *Petrol Chem Ind Int*. 2023; 6(2): 131-141. https://doi.org/10.33140/PCII.

[3] Sakthivel R, Ramesh K, Purnachandran R, Mohamed Shameer P. A review on the properties, performance and emission aspects of the third generation biodiesels. *Renew Sustain Energy Rev*. 2018; 82: 2970-2992. https://doi.org/https://doi.org/10.1016/j.rser.2017.10.037

[4] Elgharbawy AS, Sadik WA, Sadek OM, Kasaby MA. Maximizing biodiesel production from high free fatty acids feedstocks through glycerolysis treatment. *Biomass Bioenergy*. 2021; 146: 105997. https://doi.org/10.1016/j.biombioe.2021.105997

[5] Wu Z, Cai J, Liu Z, Liang X, Yu S, Nie Y. Utilization of biodiesel and glycerol for the synthesis of epoxidized acyl glycerides and its application as a plasticizer. *J Am Oil Chem Soc*. 2023; 100: 733-741. https://doi.org/10.1002/aocs.12715

[6] Hayyan A, Mjalli FS, Hashim MA, Hayyan M, AlNashef IM, Al-Zahrani SM, Al-Saadi MA. Ethanesulfonic acid-based esterification of industrial acidic crude palm oil for biodiesel production. *Bioresour Technol*. 2011; 102(20): 9564-9570. https://doi.org/10.1016/j.biortech.2011.07.074

[7] Hayyan A, Hashim MA, Hayyan M. Agro-industrial acidic oil as a renewable feedstock for biodiesel production using (1R)-(-)-camphor-10-sulfonic acid. *Chem Eng Sci*. 2013; 16(6): 223-227. https://doi.org/10.1016/j.ces.2014.03.031

[8] Sun J, Zhu W, Mu B, Zhong J, Lin N, Chen S, Li Z. Efficient extraction of biodiesel feedstock and dehydration of kitchen waste: A method based on co-dissolution of liquefied dimethyl ether and water. *Waste Manag*. 2022; 147(1): 22-29. https://doi.org/10.1016/j.wasman.2022.04.044

[9] Singh B, Srivastava AK, Prakash O. A Comprehensive Review on Rare Biodiesel Feedstock Availability, Fatty Acid Composition, Physical Properties, Production, Engine Performance and Emission. *Process Integr Optim Sustain*. 2023; 7: 1081-1116. https://doi.org/10.1007/s41660-023-00343-w

[10] Hayyan A, Yeow ATH, Abed KM, Jeffrey Basirun W, Boon Kiat L, Saleh J, Wen Han G, Chia Min P, Aljohani ASM, Zulkifli MY, Alajmi FDH, Alhumaydhi FA, Kadmouse Aldeehani A, Ali Hashim M. The development of new homogenous and heterogeneous catalytic processes for the treatment of low grade palm oil. *J Mol Liq*. 2021; 344:117574. https://doi.org/10.1016/j.molliq.2021.117574

[11] Mateos PS, Casella ML, Briand LE, Matkovic SR. Transesterification of waste cooking oil with a commercial liquid biocatalyst: Key information revised and new insights. *J. Am. Oil Chem. Soc*. 2023; 100(4): 287-301. https://doi.org/10.1002/aocs.12683

[12] Ahmed R, Huddersman K. Review of biodiesel production by the esterification of wastewater containing fats oils and grease (FOGs). *J Ind Eng Chem*. 2022; 110: 1-14. https://doi.org/10.1016/j.jiec.2022.02.045

[13] Rattanaphra D, Harvey AP, Thanapimmetha A, Srinophakun P. Kinetic of myristic acid esterification with methanol in the presence of triglycerides over sulfated zirconia. *Renew Energy*. 2011; 36(10): 2679-2686. https://doi.org/10.1016/j.renene.2011.02.018

[14] Atadashi IM, Aroua MK, Abdul Aziz AR, Sulaiman NMN. The effects of catalysts in biodiesel production. *J Ind Eng Chem.* 2013; 19(1): 14-26. https://doi.org/10.1016/j.jiec.2012.07.009

[15] Lam MK, Lee KT, Mohamed AR. Homogeneous, heterogeneous and enzymatic catalysis for transesterification of high free fatty acid oil (waste cooking oil) to biodiesel. *Biotechnol Adv*. 2010; 28(4): 500-518. https://doi.org/10.1016/j.biotechadv.2010.03.002

[16] Abdulmalek SA, Yan Y. Recent developments of lipase immobilization technology and application of immobilized lipase mixtures for biodiesel production. *Biofuels Bioprod Bioref*. 2022; 16(4): 1062-109. https://doi.org/10.1002/bbb.2349

[17] Jamil F, Saleem M, Ali Qamar O, Khurram MS, Al-Muhtaseb AH, Inayat A, Akhter P, Hussain M, Rafiq S, Yim H, Park YK. State-of-the-art catalysts for clean fuel (methyl esters) production—a comprehensive review. *J Phys Energy*. 2023; 5(1): 014005. https://doi.org/10.1088/2515-7655/aca5b3

[18] Bölük S, Sönmez Ö. Microwave-Assisted Esterification of Oleic Acid Using an Ionic Liquid Catalyst. *Chem Eng Technol*. 2020; 43(9): 1792-1801. https://doi.org/10.1002/ceat.202000045

[19] Hayyan A, Hashim MA, Hayyan M. Application of a Novel Catalyst in the Esterification of Mixed Industrial Palm Oil for Biodiesel Production. *Bioenergy Res*. 2015; 8(1): 459-463. https://doi.org/10.1007/s12155-014-9502-0

[20] Winfield DD, Moser BR. Selective hydroxyalkoxylation of epoxidized methyl oleate by an amphiphilic ionic liquid catalyst. *J Am Oil Chem Soc*. 2022; 100(3): 237-243 https://doi.org/10.1002/aocs.12672

[21] Hayyan A, Yeow ATH, Alkahli NAM, Saleh J, Aldeehani AK, Alkandari KH, Alajmi FD, Alias Y, Junaidi MUM, Hashim MA, Basirun WJ, Abdelrahman MAA. Application of acidic ionic liquids for the treatment of acidic low grade palm oil for biodiesel production. *J Ionic Liq*. 2022; 2(1): 100023. https://doi.org/10.1016/j.jil.2022.100023

[22] Hayyan A, Ali Hashim M, Mjalli FS, Hayyan M, AlNashef IM. A novel phosphonium-based deep eutectic catalyst for biodiesel production from industrial low grade crude palm oil. *Chem Eng Sci*. 2013; 92: 81-88. https://doi.org/10.1016/j.ces.2012.12.024

[23] Hayyan A, Hizaddin HF, Abed KM, Mjalli FS, Hashim MA, Abo-Hamad A, Saleh J, Aljohani ASM, Alharbi YM, Alhumaydhi FA, Ahmad AA, Yeow ATH, Aldeehani AK, Alajmi FDH, Al Nashef I. Encapsulated deep eutectic solvent for esterification of free fatty acid. *Biomass Convers Biorefin*. 2022; 12(9): 3725-3735. https://doi.org/10.1007/s13399-021-01913-z

[24] Pelit E. Synthesis of isoxazolopyridines and spirooxindoles under ultrasonic irradiation and evaluation of their antioxidant activity. *J Chem*. 2017; 2017(1).9161505. https://doi.org/10.1155/2017/9161505

[25] Zhai Y, Pan K, Zhang E. Anti-Corrosive Coating of Carbon-Steel Assisted by Polymer-Camphorsulfonic Acid Embedded Within Graphene. *Coatings*. 2020; 10(9): 897. https://doi.org/10.3390/coatings10090879

[26] Guo P. Three 2D AgI-framework Isomers With Helical Structures Controlled by the Chirality of Camphor-10-Sulfonic Acid. *Daltan Transanction*. 2011: 1716. https://doi.org/10.1039/C0DT01384F

[27] Krupińska I. The influence of aeration and type of coagulant on effectiveness in removing pollutants from groundwater in the process of coagulation. *Chem Biochem Eng Q*. 2016; 30(4): 465-475. https://doi.org/10.15255/CABEQ.2014.2016

[28] GY Han, GQ Shi, LT Qu, JY Yuan, FE Chen PW. Electrochemical Polymerization of Chiral Pyrrole Derivatives in Electrolytes Containing Chiral Camphor Sulfonic Acid. *Polymer International.* 2004*:* 53 (10): 1554-1560. https://doi.org/10.1002/pi.1597

[29] Garcia FJ, Rubio A, Sainz E, Gonzalez P, Lopez FA. Preliminary study of treatment of sulphuric pickling water waste from steelmaking by bio-oxidation with Thiobacillus ferrooxidans. *FEMS Microbiol Rev*. 1994; 14(4): 397-404. https://doi.org/10.1111/j.1574-6976.1994.tb00114.x

[30] American Oil Chemist's Society. Ca 5a-40: free fatty acids, in: Official Methods and Recommended Practices of the AOCS. 5th ed. Champaign, IL; 1998. ISBN: 978-0-935315-82-8.

[31] Park SH, Khan N, Lee S, Zimmermann K, DeRosa M, Hamilton L, Hudson W, Hyder S, Serratos M, Sheffield E. Biodiesel production from locally sourced restaurant waste cooking oil and grease: synthesis, characterization, and performance evaluation. *ACS Omega*. 2019; 4(4): 7775-7784. https://doi.org/10.1021/acsomega.9b00268

[32] Ude CN, Onukwuli OD, Ugwu BI, Okey-Onyesolu CF, Ezidinma TA, Ejikeme PM. Methanolysis optimization of cottonseed oil to biodiesel using heterogeneous catalysts. *Iran. J Chem Chem Eng*. 2020; 39(4): 355-370. https://doi.org/10.30492/ijcce.2020.43368

[33] Borugadda VB, Goud V V. Response surface methodology for optimization of bio-lubricant basestock synthesis from high free fatty acids castor oil. *Energy Sci Eng*. 2015; 3(4): 371-83. https://doi.org/10.1002/ese3.77

[34] Evans R. Verifying Model Assumptions and Testing Normality. *Vet. Surg*. 2024; 53(1). 17. https://doi.org/10.1111/vsu.14034

[35] Jia P, Lan X, Li X, Wang T. Highly Active and Selective NiFe/SiO2 Bimetallic Catalyst with Optimized Solvent Effect for the Liquid-Phase Hydrogenation of Furfural to Furfuryl Alcohol. *ACS Sustain Chem Eng*. 2018; 6(10): 13287-13295. https://doi.org/10.1021/acssuschemeng.8b02876

[36] Xie W, Gao C, Wang H. Biodiesel production from low-quality oils using heterogeneous cesium salts of vanadium-substituted polyoxometalate acid catalyst. *Catalysts*. 2020; 10(9): 1060. 1-13. https://doi.org/10.3390/catal10091060

[37] Faruque MO, Razzak SA, Hossain MM. Application of heterogeneous catalysts for biodiesel production from microalgal oil—a review. *Catalysts*. 2020; 10(9): 1025. https://doi.org/10.3390/catal10091025

[38] Ma'arof NANB, Hindryawati N, Khazaai SNM, Bhuyar P, Rahim MHAb, Maniam GP. Biodiesel (Methyl Esters). *Maejo Int. J. Energy Environ Commun*. 2021; 3(1): 30-43. https://doi.org/10.54279/mijeec.v3i1.245153

[39] Xie W, Wang H. Immobilized polymeric sulfonated ionic liquid on core-shell structured Fe3O4/SiO2 composites: A magnetically recyclable catalyst for simultaneous transesterification and esterifications of low-cost oils to biodiesel. *Renew Energy*. 2020; 145: 1709-1719. https://doi.org/10.1016/j.renene.2019.07.092

[40] Díaz L, Borges ME. Low-quality vegetable oils as feedstock for biodiesel production using k-pumice as solid catalyst. Tolerance of water and free fatty acids contents. *J Agric Food Chem*. 2012; 60(32): 7928-3793. https://doi.org/10.1021/jf301886d

[41] Khor CP, Jaafar M bt, Ramakrishnan S. Optimization of Conductive Thin Film Epoxy Composites Properties Using Desirability Optimization Methodology. *J Optim*. 2016: 652928. 1652928. https://doi.org/10.1155/2016/1652928

[42] Loryuenyong V, Kaewmanee S, Rattanawaraporn S, Chimplenapanon N, Buasri A. Optimization of microwave-assisted biodiesel production using Iron (III) oxide - Calcium oxide / Activated charcoal derived from waste Asian green mussel shell as heterogeneous catalyst. *IOP Conf Ser Mater Sci Eng*. 2023; 1280(1): 012004. https://doi.org/10.1088/1757-899x/1280/1/012004

[43] Melchiorre M, Amoresano A, Budzelaar PHM, Cucciolito ME, Mocerino F, Pinto G, Ruffo F, Tuzi A, Esposito R. Parts-Per-Million (Salen)Fe(III) Homogeneous Catalysts for the Production of Biodiesel from Waste Cooking Oils. *Catal Letters*. 2022; 152(12): 3785-3794. https://doi.org/10.1007/s10562-022-03948-x

[44] Betiku E, Etim AO, Pereao O, Ojumu TV. Two-Step Conversion of Neem (Azadirachta indica) Seed Oil into Fatty Methyl Esters Using a Heterogeneous Biomass-Based Catalyst: An Example of Cocoa Pod Husk. *Energy Fuels*. 2017; 31(6): 6182-6193. https://doi.org/10.1021/acs.energyfuels.7b00604

[45] Chai M, Tu Q, Lu M, Yang YJ. Esterification pretreatment of free fatty acid in biodiesel production, from laboratory to industry. *Fuel Process. Technol*. 2014; 125: 106-113. https://doi.org/10.1016/j.fuproc.2014.03.025

[46] Okpalaeke KE, Ibrahim TH, Latinwo LM, Betiku E. Mathematical Modeling and Optimization Studies by Artificial Neural Network, Genetic Algorithm and Response Surface Methodology: A Case of Ferric Sulfate-Catalyzed Esterification of Neem (Azadirachta indica) Seed Oil. *Front Energy Res*. 2020; 8(November): 1-14. https://doi.org/10.3389/fenrg.2020.614621

[47] Anil N, Rao PK, Sarkar A, Kubavat J, Vadivel S, Manwar NR, Paul B. Advancements in sustainable biodiesel production: A comprehensive review of bio-waste derived catalysts. *Energy Convers Manag*. 2024; 318: 118884. https://doi.org/https://doi.org/10.1016/j.enconman.2024.118884

[48] Pasha MK, Dai L, Liu D, Guo M, Du W. An overview to process design, simulation and sustainability evaluation of biodiesel production. *Biotechnol Biofuels*. 2021; 14(1): 1-24. https://doi.org/10.1186/s13068-021-01977-z

[49] Kokanović A, Ajdačić V, Terzić Jovanović N, Stankic S, Opsenica IM. Pd Nanoparticles Supported on Ultrapure ZnO Nanopowders as Reusable Multipurpose Catalysts. *ACS Appl Nano Mater*. 2023; 6(17): 15820-15828. https://doi.org/10.1021/acsanm.3c02743

[50] Rathore D, Sevda S, Prasad S, Venkatramanan V, Chandel AK, Kataki R, Bhadra S, Channashettar V, Bora N, Singh A. Bioengineering to Accelerate Biodiesel Production for a Sustainable Biorefinery. *Bioeng*. 2022; 9(11): 618. 1ttps://doi.org/10.3390/bioengineering9110618

[51] Alhomaidi E, Aljabri M, Alsharari SS, Alsam A. Chromatographic assessment of biodiesel production from Peganum harmala seed oil using environmentally benign nano-catalysts. *Biomed Chromatogr*. 2024; 38(3): e5794. https://doi.org/10.1002/bmc.5794

[52] Oloyede CT, Jekayinfa SO, Alade AO, Ogunkunle O, Otung NAU, Laseinde OT. Exploration of agricultural residue ash as a solid green heterogeneous base catalyst for biodiesel production. *Eng Rep*. 2023; 5(1): 1-23. https://doi.org/10.1002/eng2.12585

Primena metoda površine odgovora za optimizaciju procesa visoke konverzije slobodnih masnih kiselina korišćenjem (1R)-(-)-kamfor-10-sulfonske kiseline i gvožđe(III) sulfata

Adeeb Hayyan[1,2], Khalid M. Abed[1,3], Mohammed A. Al-Saadi[4], Amal A. M. Elgharbawy[5,6], Yousef Mohammed Alanazi[7], Jehad Saleh[7], Nur Hanie Mohd Latiff[8], Sharifah Shahira Syed Putra[9], Mohd Roslan Mohd Nor[10] i Shareef Fadhil Mahel Alhashemi[11]

[1]*Department of Chemical Engineering, Faculty of Engineering, Universiti Malaya, Kuala Lumpur, Malaysia*
[2]*Sustainable Process Engineering Centre (SPEC), Faculty of Engineering, Universiti Malaya, Kuala Lumpur, Malaysia*
[3]*Department of Chemical Engineering, College of Engineering, University of Baghdad, Baghdad, Iraq*
[4]*National Chair of Materials Science and Metallurgy, University of Nizwa, Nizwa, Oman*
[5]*International Institute for Halal Research and Training (INHART), International Islamic University Malaysia, Kuala Lumpur, Malaysia*
[6]*Bioenvironmental Engineering Research Centre (BERC), Department of Biotechnology Engineering, Faculty of Engineering, International Islamic University Malaysia (IIUM), Kuala Lumpur, Malaysia*
[7]*Department of Chemical Engineering, College of Engineering, King Saud University, Riyadh, Saudi Arabia*
[8]*Global Centre for Environmental Remediation (GCER), College of Engineering, Science, and Environment (CESE), University of Newcastle, Callaghan, Australia*
[9]*Faculty of Industrial Sciences and Technology, Universiti Malaysia Pahang Al-sultan Abdullah, Lebuhraya Tun Abdul Razak, 26300 Gambang, Pahang, Malaysia*
[10]*Halal Research Group, Academy of Islamic Studies, Universiti Malaya, Kuala Lumpur, Malaysia*
[11]*Department of Chemistry, College of Science, Sultan Qaboos University, Muscat, Oman*

(Naučni rad)

Izvod

U radu je izvršeno ispitivanje proizvodnje biodizela iz kiselog sirovog palminog ulja korišćenjem jednog homogenog katalizatora, (1R)-(-)-kamfor-10-sulfonske kiseline (10-CSA) i jednog heterogenog katalizatora, gvožđe(III) sulfata, sa aspekta njihove katalitičke aktivnosti, mogućnosti recikliranja i optimizacije procesa primenom metode odgovora površine. Optimalni uslovi su identifikovani korišćenjem Bok-Behnken faktorskog dizajna. Za 10-CSA, optimizovani uslovi su dali smanjenje slobodnih masnih kiselina (FFA) na 0,43 mas.%, sa dozom katalizatora od 1,5 mas.% (ispitani opseg: 1,0-2,0 mas.%), molarnim odnosom metanola i ulja od 12,60 g do 1:1:1 (umereno temperaturno područje), temperaturom od 59,6 °C (ispitani opseg: 50 do 65 °C), i vremenom reakcije od 33,1 min (ispitani opseg: 30 do 40 min). Za gvožđe(III) sulfat, optimizovani uslovi su doveli do smanjenja FFA na 1,04 mas.%, sa dozom katalizatora od 3,14 mas.% (ispitani opseg: 2,5 do 3,5 mas.%), molarnim odnosom metanola i ulja od 12:1 (ispitani opseg temperature od 1:10°C), temperaturom reakcije od 60 °C (ispitani opseg: 55 do 70 °C), i vreme reakcije od 178,6 min (ispitani opseg: 150 do 180 min). Rezultati ANOVA analize su potvrdili značaj ključnih faktora za oba katalizatora (p <0,05), sa vrednostima R^2 od 0,937 za 10-CSA i 0,916 za gvožđe(III) sulfat, što ukazuje na dobro uklapanje modela. Srednja relativna procentna devijacija bila je <5 % za oba modela, što pokazuje visoku tačnost predviđanja. Utvrđeno je da je nedostatak uklapanja beznačajan (p >0,05), što potvrđuje adekvatnost modela. Oba katalizatora su postigla visoku konverziju FFA od 95,2 % za 10-CSA i 88,2 % za gvožđe(III) sulfat, što ispunjava standarde EN 14214 i ASTM D6751. Značajno je da je 10-CSA pokazao bolju katalitičku aktivnost i mogućnost recikliranja, čime se ističe njegov potencijal za proizvodnju biodizela u industrijskim razmerama. Ova studija nudi praktičan uvid u optimizaciju procesa esterifikacije za proizvodnju biodizela iz kiselog sirovog palminog ulja.

Ključne reči: kiselo sirovo palmino ulje; biodizel; esterifikacija; homogeni kiseli katalizator; heterogeni kiseli katalizator